

READ: Reliability-Enhanced Accelerator Dataflow Optimization using Critical Input Pattern Reduction

Zuodong Zhang^{1,3}, Renjie Wei¹, Meng Li^{2,1*}, Yibo Lin^{1,3,4}, Runsheng Wang^{1,3,4}, and Ru Huang^{1,3,4}

¹School of Integrated Circuits, Peking University, Beijing, China

²Institute for Artificial Intelligence, Peking University, Beijing, China

³Institute of Electronic Design Automation, Peking University, Wuxi, China

⁴Beijing Advanced Innovation Center for Integrated Circuits, Beijing, China

Abstract—With the rapid advancements of deep learning in recent years, hardware accelerators are continuously deployed in more and more safety-critical applications such as autonomous driving and robotics. While the accelerators are usually fabricated with advanced technology nodes for high performance and energy efficiency, they are also more prone to timing errors under process, voltage, temperature, and aging (PVTa) variations. By revisiting the physical sources of timing errors, we show that most of the timing errors in the accelerator are caused by a specific subset of input patterns, defined as critical input patterns. To improve the timing error resilience of the accelerator, in this paper, we propose READ, a reliability-enhanced accelerator dataflow optimization technique that can effectively reduce timing errors. READ reduces the occurrence of critical input patterns by exploring the optimal computing sequence when mapping a trained deep neural network to accelerators. READ only changes the order of multiply-accumulate operations in a convolution, which introduces negligible hardware overhead and no impact on accuracy. The experimental results on VGG and ResNet demonstrate on average $7.8\times$ timing error rate (TER) reduction and up to $37.9\times$ TER reduction for certain layers. The results also show that READ enables the accelerator to maintain accuracy over a wide range of PVTa variations, making it a promising approach for robust deep-learning design.

I. INTRODUCTION

Deep neural networks (DNNs) have revolutionized different applications ranging from computer vision to natural language processing, and are widely deployed in data centers and edge devices. It can be foreseen that DNNs will be applied in more and more safety-critical applications like autonomous driving and robotics, which typically require highly reliable computing to avoid catastrophic consequences. Therefore, not only the model’s robustness against various perturbations like adversarial noise, but also the robustness of the silicon-based accelerators to hardware faults need to be comprehensively investigated [1], [2], [3], [4].

As the fabrication of DNN accelerators pushes toward nanoscale, the transient errors like timing errors that cannot be detected during manufacturing tests have become a more pronounced problem [5]. Timing errors due to the increased path delay usually occur under process, voltage, temperature, and aging (PVTa) variations. Although DNN shows inherent error resilience at the algorithm level, timing errors are shown

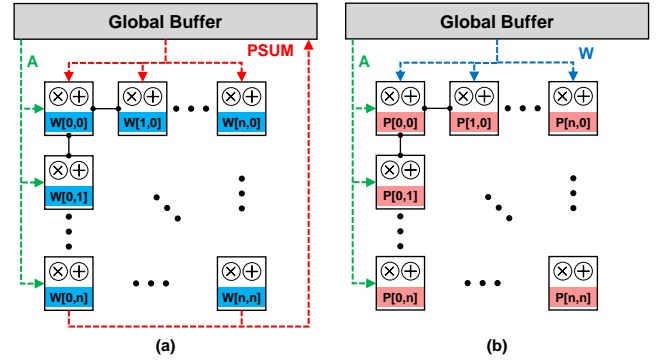


Fig. 1: Dataflow for 2-D spatial accelerators. (a) Weight stationary. (b) Output stationary.

to cause significant accuracy degradation [6], [7], [8]. This is because, on one hand, timing errors often occur in the most significant bit; while on the other hand, the error will accumulate in each convolution operation and across the whole network [8].

Several timing error-resilient accelerator designs have been explored from the architecture level to the circuit level. These works either utilize timing error detection and correction (TEDC) schemes to recover the correct value [7], [9], [10], [6], or algorithm-based fault tolerance (ABFT) techniques to check the correctness of computing [11], [12]. However, these approaches usually compromise network accuracy or introduce large hardware overhead.

In this paper, we provide a promising solution to alleviate the timing error in DNN accelerators from a new perspective. We propose READ, a reliability-enhanced accelerator dataflow optimization technique, which can improve the timing error resilience of DNN accelerators by exploring the optimal computing sequence. To the best of our knowledge, READ is the first work that mitigates the accuracy loss of DNN accelerators due to timing errors by exploiting sequence optimization of dataflow, and it is orthogonal to the previous TEDC and ABFT approaches. The major contributions of this work are as follows:

- 1) We observe that timing errors are highly input pattern dependent and a subset of input patterns are significantly

*Corresponding author: meng.li@pku.edu.cn

more vulnerable. The observation provides a new opportunity for timing error reduction by avoiding these critical patterns.

- 2) We develop READ, a reliability-enhanced dataflow optimization technique to reduce timing errors in the multiply-accumulate (MAC) datapath. READ reduces the critical input patterns by weight re-ordering with negligible hardware overhead and no accuracy loss.
- 3) We propose a clustering algorithm that divides the weight matrix into sub-matrices to improve the reordering flexibility and achieves better reordering results.
- 4) The experimental results demonstrate on average $7.8\times$ timing error rate (TER) reduction and up to $37.9\times$ TER reduction for certain layers, which enables the accelerator to maintain accuracy over a wide range of PVT variations.

The rest of this paper is organized as follows. Section II introduces the background of DNN accelerators and the reliability concerns in DNN accelerators. Section III introduces the motivation of the proposed optimization method. Section IV presents details of the algorithm. Section V demonstrated the experimental results of our algorithm. Finally, Section VI concludes the paper.

II. BACKGROUND

A. Spatial DNN Accelerators

DNN accelerators aim to speed up the computationally expensive operations in DNN inference, e.g., computing the matrix multiplication $W \times A$. The 2-D spatial accelerators are a promising direction because of their capability to support parallel processing with minimal data movement [17], [18], [19]. The 2-D spatial accelerators usually comprise the following major components: a two-dimensional arithmetic computing array, a network-on-chip for operand access and delivery, control blocks, and on-chip memory.

To reduce access to external memory, specialized processing dataflows are designed to enable data reuse across different process units. The dataflow dictates what data gets read into the memory hierarchy and how data are propagated in the computing array. Representative dataflows include weight stationary, and output stationary [20].

Fig. 1 gives a schematic of weight stationary and output stationary. The weight stationary dataflow [19], [18] is designed to minimize the movement of the weights. Each weight is read from the buffer into the register file (RF) of each PE and stays stationary, and the inputs and partial sums must move through the spatial array and global buffer. The output stationary dataflow is designed to minimize the partial sums movement. It keeps the accumulation of partial sums for the same output activation value local in the RF, stream the input activations across the PE array, and broadcast the weights to all PEs in the array [17].

If the size of matrix-matrix multiplication is larger than the computing array, the total weight matrix will be tiled into sub-matrices and be performed in several blocks.

B. Reliability Concerns in Accelerator

The transient errors in silicon-based accelerators can be divided into two categories, depending on where they occur. The first is the soft errors that occur in the memory or on-chip buffers, and the second category is the timing errors that occur in the processing element (PE) [7]. The memory and on-chip buffers are usually protected with the error correction code (ECC), therefore, we mainly focus on timing errors. The timing path of accelerators can be roughly divided into the timing path inside the computing array and the timing path between the computing array and the local cache for data exchange. Among them, the timing path inside the computing core is more critical. Previous works [6], [21], [8] have also demonstrated that the accuracy of DNN can be very sensitive to timing errors in computing array because of the following reasons: 1) the timing errors usually occur at the most significant bit, which is catastrophic for the computing results; 2) timing errors may occur in every single MAC operation, while thousands of MAC operations are required to compute a single output activation in the convolution layer. The bit error rate (BER) of the output activation can be estimated by the TER of MAC as below:

$$BER(i) = 1 - \prod_{i=1}^N (1 - TER(i)) \quad (1)$$

where N is the number of MAC operations required for an output activation. Even if the TER of a single MAC operation is relatively small, the BER of the output activations can be large. Therefore, the inference accuracy will decrease rapidly with the increase of timing errors.

At the same time, accelerators fabricated with advanced technology nodes are more prone to timing errors under PVT variations [22]. Thus the conventional guardbanding will not only result in excessive performance loss, but also cannot guarantee the requirements in safety-critical scenarios. All these reliability concerns aggregate the uncertainty of the deep learning processing and hinder the deployment of deep learning in safety-critical applications.

C. Related Works

To improve the timing error resilience of accelerators, a number of approaches from algorithm-layer to circuit-layer have been proposed. We summarize the features of the representative state-of-the-art reliability-enhanced techniques in Table I. The algorithm-layer techniques utilize the NN's inherent redundancy and tolerance for errors, and common methods include sensitivity analysis, fault/noise-tolerant training, and model architecture design. Libano et al. conduct layer-wise sensitivity analysis and protect the vulnerable layer [14]. Schorn et al. propose a training strategy to adjust neuron sensitivities [13], which argues that achieving a homogeneous resilience distribution can help DNN robustness. Zhao et al. adopt the algorithm-based fault tolerance (ABFT) technique of error-tolerant matrix-matrix multiplication for convolution

TABLE I: Features of the representative state-of-the-art timing error-resilient spatial accelerator design methods.

Methods	Layer	Scalable with Technology	Accuracy Loss	Hardware Overhead	Throughput Drop	Design Effort
Guardbanding	circuit-layer	no	no	High	yes	Low
Sensitivity analysis [13], [14]	algorithm-layer	yes	yes	Negligible	no	Medium
ABFT [11], [12]	algorithm-layer	yes	no	Medium	yes	High
Timing error detection [7], [15], [6]	circuit-layer	yes	no	High	no	Medium
Timing error prediction [10], [16]	circuit-layer	yes	yes	Medium	no	High
Ours	dataflow	yes	no	Negligible	no	Low

operations to obtain the error detection/correction capability [11], and Filippas et al. further proposed a lightweight ABFT implementation [12].

Circuit-layer techniques usually utilize timing error detection (using Razor flip-flops [23], for instance) and correction approaches. Zhang et al. introduced a new timing speculation methodology for accelerators, in which the MAC unit encountering a timing error, will steal an execution cycle from its downstream MAC to recover the correct value [7]. Gundi et al. further improved the correction scheme [15]. Whatmough et al. proposed a scheme that utilizes lightweight Razor flip-flops and circuit-layer timing borrowing to tolerate the timing errors [6].

To the best of our knowledge, READ is the first one that exploits the impact of dataflow on timing errors, and does not need any hardware modification in the computing array. Moreover, READ is a post-training optimization technique, so most algorithm-layer techniques are orthogonal to READ, and READ can be also deployed on the timing speculation accelerator to reduce the toggle rate of TEDC modules, and enable more aggressive voltage scaling for higher energy efficiency.

III. MOTIVATION: CRITICAL PATTERN REDUCTION

We first analyze the factors affecting the TER in spatial accelerators. For a specific cycle, the factors that determine whether a timing error will occur fall into two categories: 1) the input pattern which determines the triggered paths; 2) the operation conditions (including but not limited to temperature, voltage, and aging) that affect the path delay of these triggered paths. The fluctuation of the operating conditions is often uncontrollable and only a small set of paths may exceed the clock cycle, i.e. critical paths. Therefore, to reduce the timing error rate, we focus on reducing the trigger rate of the critical paths.

The basic PE is the MAC unit. We use the MAC unit in TPU as an example, which contains an 8-bit multiplier and a 24-bit accumulator. Through performing dynamic timing analysis of the synthesized MAC unit, we find that the most common type of critical input pattern is the input that can cause the sign bit flip of partial sum (PSUM). For example, when computing $3 \times (-2) + 2 = -4$ in a certain MAC, the 2's complement representation is $00000011 \times 11111110 + 00000000000000000000010 = 111111111111111111111100$. The flip of the sign bit triggers the long carry chain of the accumulator, and thus, triggers the

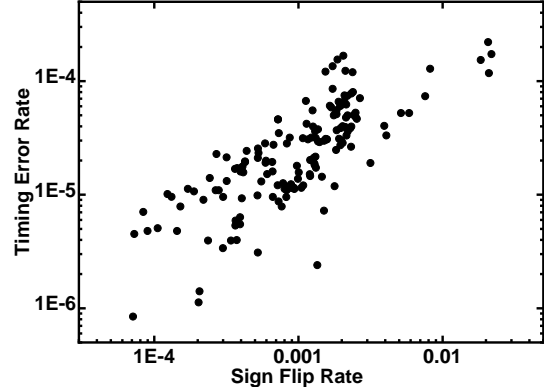


Fig. 2: The sign flip rate and the timing error rate demonstrate a strong correlation.

TABLE II: Notations used in this paper.

N, H, W, K	Output batch, height, width, channel
C, F_x, F_y	Input channel, filter height, filter width
A_r, A_c	Rows and columns of the systolic array
W	Weight matrix
S	Sequence of input channel
T	Cluster of output channel

timing critical paths. Similarly, it is also possible to trigger critical paths when PSUM changes from negative to positive.

To further validate this observation, we collect the sign flip rate and TER from different MAC units running different convolution layers with different dataflow. As shown in Fig. 2, the sign flip rate and the TER demonstrate a strong correlation, which indicates that most of the timing errors are caused by the sign flip of PSUM. Hence, to minimize the TER, an effective approach is to reduce the sign flip rate of PSUM.

IV. METHODOLOGY

In this section, we will formulate the problem of critical pattern reduction and propose a set of optimization techniques to reduce critical patterns and TER. We summarize the notations used in the paper in Table II.

A. Problem Formulation

PSUM is the intermediate accumulation result of a convolution operation, and the sign bit flip means that the sign bit of PSUM is different in two adjacent cycles. The total number

of sign bit flips computing an output activation is calculated as:

$$SF = \sum_{j=0}^{C-1} \text{sign}\left(\sum_{i=0}^j a_i w_i\right) \oplus \text{sign}\left(\sum_{i=0}^{j+1} a_i w_i\right)$$

where \oplus denotes the XOR operation and $\text{sign}(\cdot)$ extracts the sign bit of the input, which returns 1 when the input is positive and returns 0 for negative inputs.

The optimization problem is combinatorial and the computation complexity scales exponentially, which quickly becomes intractable for even small-size problems. To efficiently solve the problem above, we make the following two observations:

- As rectified linear unit (ReLU) is widely used in modern networks, the input activations a_i of a convolution layer are often non-negative. Hence, the sign of each MAC result is mainly determined by the sign of weight w_i and the sign flip of PSUM is mainly determined by the sequence of weights for the computation. Fig. 3 gives a simple example to show how weight sequence impacts the sign flip.
- As the PSUM is usually initialized to 0, the minimum number of sign flips for when computing an output is 0 or 1, depending on whether the final activation is positive or negative.

Based on the observations above, we propose the following heuristic solution for the optimization above: *when computing an output activation, arrange the computation sequence so that all MACs with non-negative weights are computed first.* The proposed solution has two main properties:

- Compute correctness: as the convolution operation is independent of the computing order, changing the order of MAC operations only affects the value of PSUMs but not the final output activation.
- Sign flip optimality: Given non-negative inputs, after arranging the weights, the value of PSUM will first increase monotonically, and then monotonically decrease. If the final output activation is non-negative, PSUM is always non-negative, and no sign flip occurs (shown in Fig. 3 (b)). If the final output activation is negative, PSUM will become negative and the sign flip occurs once (shown in Fig. 3 (c)).

B. Input Channel Reordering

We use the systolic array, the most widely used 2-D accelerator, with output stationary dataflow as an example to illustrate the algorithm. It should be noted that the algorithm proposed can be easily extended to other dataflow or 2-D spatial accelerators with minor modifications.

Fig. 4 gives an example of mapping a 1-by-1 convolution to a systolic array with the output stationary dataflow. The weights are streamed along the row direction and the input activations are propagated in the column direction. Each MAC unit is responsible for all the computations required for a pixel in the output feature map.

The heuristic solution proposed above can find the optimal sequence for the case of a single output channel. However, to

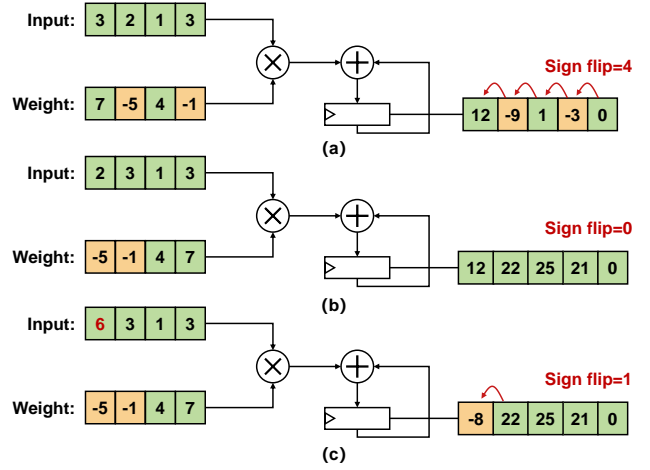


Fig. 3: A 1×4 convolution calculated in different orders. Reordering weights does not change the computing result, but avoids the critical input pattern of MAC.

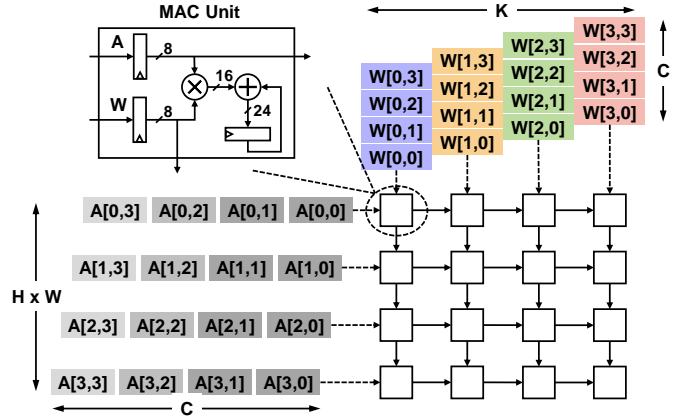


Fig. 4: The architecture of a systolic array-based DNN accelerator with the output stationary dataflow.

improve throughput and data reuse, systolic arrays often have more than one column to process multiple output channels simultaneously. To reduce the sign flip of simultaneously processed channels, we need to find a sequence suitable for all these output channels. Hence, we define the input channels reordering problem as below.

Problem 1 (Input Channel Reordering) Given a weight matrix $W \in \mathbb{R}^{C \times K}$, divide the W into n sub-matrices $W_1, \dots, W_n \in \mathbb{R}^{C \times A_c}$ according to the size of systolic array, and find the optimal S_1^*, \dots, S_n^* for each sub-matrix such that the sign flip of PSUM during the computing is minimized.¹

To efficiently solve the reordering problem, we propose two sorting algorithms as described in Algorithm1. The first algorithm sorts the input channels according to the number of non-negative weights in each channel. If two channels have the same number of non-negative weights, the channel with a larger sum of weights is ranked in the front. We denote

¹We assume $F_x = F_y = 1$ for the weight matrix in formulation and algorithm, but the definition and analysis can be easily extended to cases where F_x and F_y are larger than 1.

Algorithm 1: Input channel reorder.

Input: Weight matrix W **Output:** Sequence S of each sub-matrix

```
1 Function sort_input_channel (matrix  $W$ ):
2   for  $i = 1 : C$  do
3      $metric\_sign[i] = \sum_{j=1}^{A_c} sign(W[i, j]);$ 
4      $metric\_mag[i] = \sum_{j=1}^{A_c} W[i, j];$ 
5     if  $sorting\_criteria == "sign\_first"$  then
6        $scale\ metric\_mag$  to between 0 to 1;
7     else
8        $scale\ metric\_sign$  to between 0 to 1;
9      $metric\_sorting = metric\_sign + metric\_mag;$ 
10     $S = argsort(metric\_sorting);$ 
11    return  $S;$ 
12 Divide  $W$  into  $n$  sub-matrix  $W_1, \dots, W_n;$ 
13 for  $i = 1 : n$  do
14    $S_i = sort\_input\_channel(W_i);$ 
15   reorder sub-matrix  $W_i$  in order  $S_i;$ 
16   reorder input activations in order  $S_i;$ 
```

this method as the *sign_first* approach. The Second algorithm sorts the input channels according to the sum of weights in each channel. If the sums of two channels are the same, the channel that has more non-negative weights is ranked in front. We denote this method as the *mag_first* approach.

We use a convolution layer of the VGG-16 on the Cifar10 dataset as an example and run the two reordering algorithms. Fig. 5 (a) shows the proportion of negative and non-negative weights in different positions of the initial weight matrix. It can be seen that the distribution of non-negative and negative weights is uniform. Fig. 5 (b) and (c) show the proportion for the reordered weight matrix, in which the non-negative weights concentrate in the front and the negative weights are mainly distributed in the back. And the reordering results of the *sign_first* approach are better.

C. Output Channel Clustering

To further improve the effectiveness when the number of columns A_c is large, we propose to cluster the output channels first before segmenting the weight matrix. Then, the input channels are reordered for each cluster separately. We denote this approach as *cluster-then-reorder*. Consider the example of the following weight matrix:

$$W = \begin{bmatrix} 4 & -5 & 5 & -1 \\ -10 & 3 & -2 & 2 \\ 9 & -2 & 3 & -1 \\ -2 & 3 & -6 & 3 \end{bmatrix}$$

Assume the computing array has 2 columns and only allows for streaming 2 output channels simultaneously. Instead of directly segmenting W , we can first cluster the output channels into 2 groups, i.e., 0, 2 and 1, 3, and then segment W into W_1 and W_2 as below:

$$W_1 = \begin{bmatrix} 4 & 5 \\ -10 & -2 \\ 9 & 3 \\ -2 & -6 \end{bmatrix}, W_2 = \begin{bmatrix} -5 & -1 \\ 3 & 2 \\ -2 & -1 \\ 3 & 3 \end{bmatrix}$$

Compared to direct segmenting, we can assign output channels with similar sign positions to the same cluster, which makes it easier to reorder each sub-matrix.

To formulate the clustering problem, we first define the sign difference (SD) between two n -dimensional vectors x and y as the Manhattan distance of two vectors:

$$SD(x, y) = \sum_{i=1}^n |sign(x[i]) - sign(y[i])|$$

Let T_1, \dots, T_n denote the n clusters of output channels, and W_{T_1}, \dots, W_{T_n} denote the corresponding n sub-matrices. Similarly, the SD of a sub-matrix W_{T_i} can be defined as

$$SD(W_{T_i}) = \sum_{i, j \in T_i} SD(W_{T_i}[:, i], W_{T_i}[:, j])$$

The smaller the SD is for a sub-matrix, the easier it is to reorder the input channels and reduce sign bit flips. Hence, the output channel clustering problem can be defined as follows.

Problem 2 (Output Channel Reordering) Given a weight matrix $W \in \mathbb{R}^{C \times K}$, find n clusters T_1, \dots, T_n such that the sign difference of each sub-matrix W_{T_i} is minimized, i.e.,

$$\begin{aligned} \min_{T_1, \dots, T_n} & \sum_{i=1}^n SD(W_{T_i}) \\ \text{s.t.} & T_i \cap T_j = \emptyset \quad \forall i \neq j \\ & \bigcap_{i=1}^n T_i = \{1, \dots, K\} \end{aligned}$$

This is a hard-balanced clustering problem, which can be solved by many proven algorithms. We adopt the balanced KNN on the weight sign matrix by the Manhattan metric to solve this problem.

The convergence plot of the clustering algorithm is shown in Fig. 5 (d). We found that the clustering algorithm further concentrates the non-negative weights into the front of the matrix and converges very well.

D. Hardware Support

The input channel reordering algorithm switches the weight matrices and input sequences. While the weight matrices can be reordered before inference, the input activations have to be reordered during inference. This is because we use different input sequences for different clusters of output channels. As shown in Fig 6, the reordering can be realized by simply augmenting the activation read logic with an address lookup table (LUT) to enable accessing reordered activations. For a layer with 1024 channels, the required LUT SRAM size is less than 2KB. Compared to the original on-chip buffer (usually 2~64MB), the energy and area overhead of LUT are negligible.

Output channel clustering will change the order of output activations, hence it impacts the memory fetching of the next

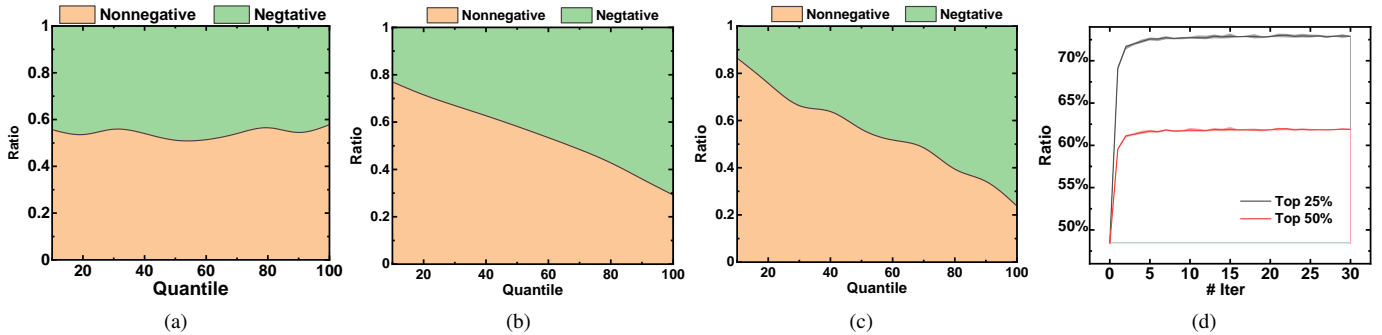


Fig. 5: The proportion of negative and non-negative weights in different positions of (a) the initial weight matrix, (b) the weight matrix reordered by the *mag_first* approach, and (c) the weight matrix reordered by the *sign_first* approach. (d) The ratio of non-negative weights in the top 25% and 50% of the weight matrix.

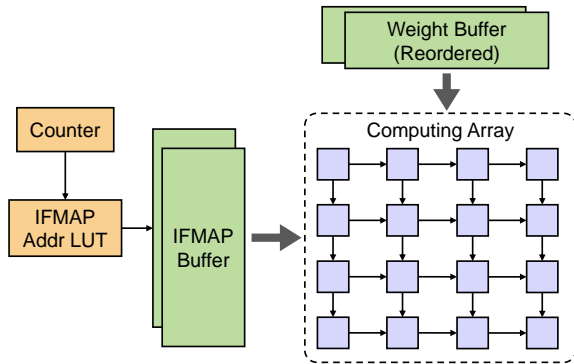


Fig. 6: Hardware support for the proposed technique.

layer. As the reordering algorithm across layers proposed in [24], starting from the second layer, memory fetching of input activations of each layer is determined by two orders: the weight order of the current layer, applied along its C dimension, and the output channel order of the previous layer, applied along its K dimension.

The proposed algorithm only changes the order of computing, without introducing any additional computation. Moreover, as the computing order is determined before inference, the process of writing to LUT SRAM can be implemented concurrently with the writing of weights and input activations, without affecting the throughput. Additionally, as the size of the LUT SRAM is small, the impact on bandwidth is negligible.

V. EXPERIMENTAL RESULTS

A. Experimental Setup

We use VGG-16 and ResNet-18 trained on the CIFAR10 and CIFAR100 dataset, and pre-trained ResNet-34 on ImageNet for evaluation. We designed an output-stationary systolic array with 16 rows and 4 columns. Each MAC unit in the array can support the multiplication and accumulation of 8-bit activations, 8-bit weights, and 24-bit partial sums. The array is synthesized with the open-source Nangate 15nm standard cell library [25], using Synopsys Design Compiler. The nominal frequency is determined by the static timing

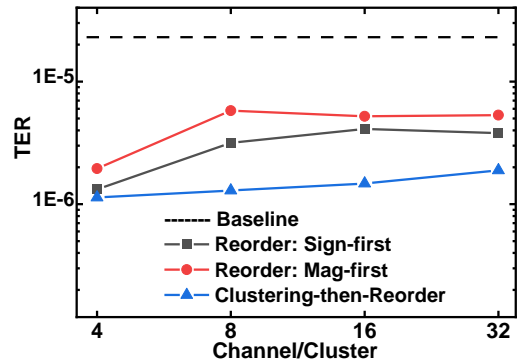


Fig. 7: TER with different reordering algorithms for different channels per cluster.

analysis with Synopsys Primetime. TER of MAC units under PVTa variations is evaluated by the dynamic timing analysis framework proposed in [26]. For voltage and temperature fluctuation, we use SiliconSmart to generate the LVF libraries at nominal, 3%, and 5% VT fluctuation with a commercial 16/14 nm FinFET modelcard. For aging analysis, we consider the negative bias temperature instability (NBTI) as NBTI dominates the transistor aging in digital circuits [27]. The baseline results are from the same architecture as the original computation sequence.

B. Layer-wise TER Reduction

We first compare the layer-wise TER of different algorithms. The TER is estimated by assuming 10-year aging and 5% voltage and temperature fluctuation. The results are shown in Fig. 7, although reordering algorithms become less effective as the number of array columns A_c increases, there is a significant reduction in the TER compared to the baseline without reordering. Moreover, the *sign_first* approach achieves a larger TER reduction compared to *mag_first*, probably because most of the weights are small. Compared to direct reordering, the *cluster-then-reorder* algorithm performs better, especially when the number of columns A_c is relatively large. Therefore, unless specifically mentioned in the rest of the paper, the reordering algorithm used is the *sign_first* approach.

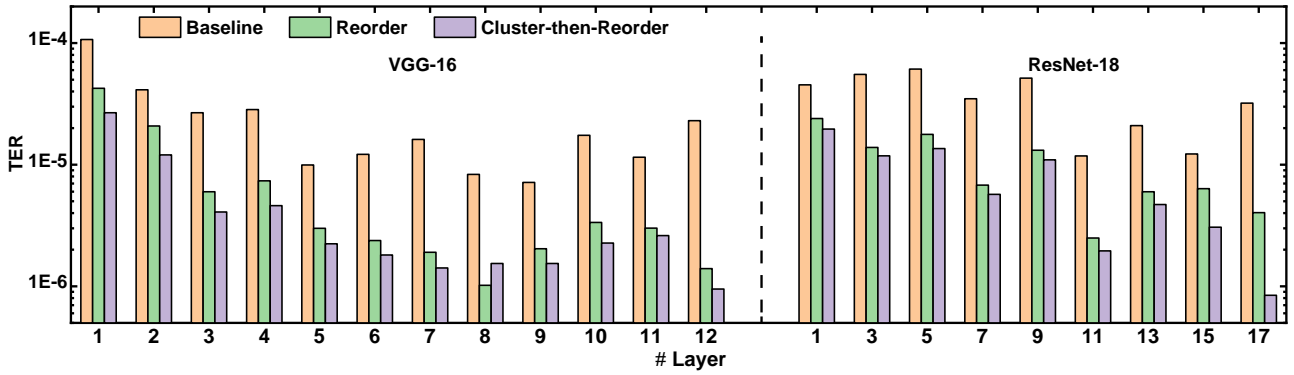


Fig. 8: Timing error rate comparison for different reliability-enhanced algorithms on ResNet-18 and VGG-16.

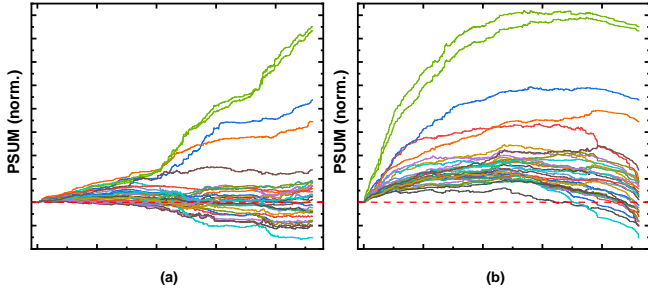


Fig. 9: The accumulation of PSUM in convolution in (a) original sequence and (b) reordered sequence.

As shown in Fig. 8, the average TER reduction of the direct reordering and the cluster-then-reorder algorithms are $4.9\times$ and $7.8\times$, respectively. The *cluster-then-reorder* algorithm usually results in a higher reduction for most of the layers, and it has better performance in the later layers of the network since the number of output channels is larger in the later layers.

Fig. 9 gives a fine-grained view to show how reordering can reduce timing errors. We show the accumulation of PSUM during multiple convolutions on a MAC when running VGG-16. Because the algorithm puts the positive weights in the front, the PSUM will increase first and then decrease (Fig. 9 (b)), which significantly reduces the number of sign flips (through the red dash line). Fig. 9 also indicates that by adopting the proposed reorder technique, the sign flip rate of PSUM for a specific NN layer is also determined by the proportion of the negative value in output activations of the current layer. The smaller the proportion of negative output activations, the lower timing error rate.

Moreover, we observed that the TER reduction of a certain layer is related to the distribution and sparsity of the weights. Layers with a higher proportion of non-negative weights tend to have more ordered sorting weights, and result in better TER reduction. We also found that weight matrices with higher sparsity tend to cluster and sort more easily. The proposed method did not perform well due to high proportions of negative weights in certain layers. But the proposed method achieved a significant reduction in error rate across all tested layers. These results suggest that the TER can be further

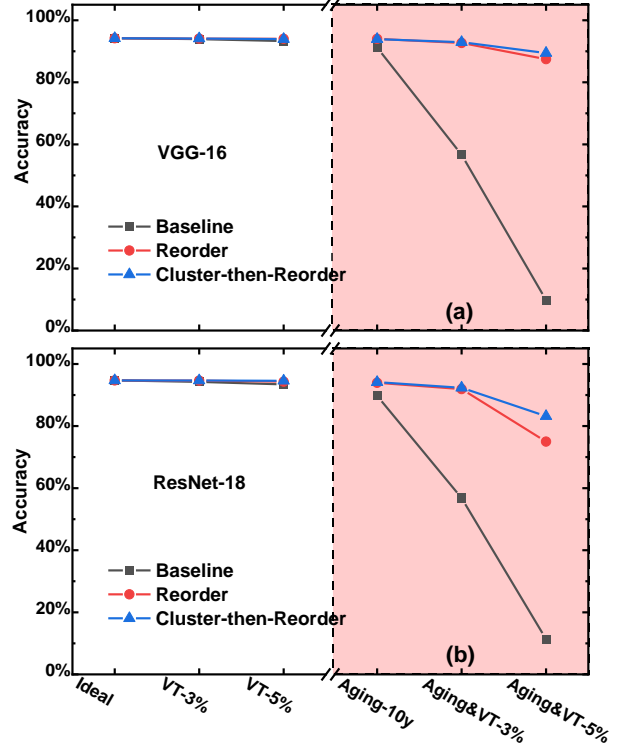


Fig. 10: Accuracy of (a) VGG-16 and (b) ResNet-18 on Cifar10 dataset under various PVTa conditions with different optimization techniques.

improved by adjusting the weight matrix according to certain rules during training.

C. Accuracy Improvement

After obtaining the layer-wise TERs, we use the equation 1 to calculate the BERs of the output activations. Then, we perform an error-injection simulation to evaluate the inference accuracy [21]. The error-injection simulation is implemented using PyTorch. We randomly flip the corresponding bits of the output activations (before the activation function) according to the BERs. To avoid randomness error, the batch size is set to 128 and the error-injection simulation is repeated five times with different seeds for each BER combination.

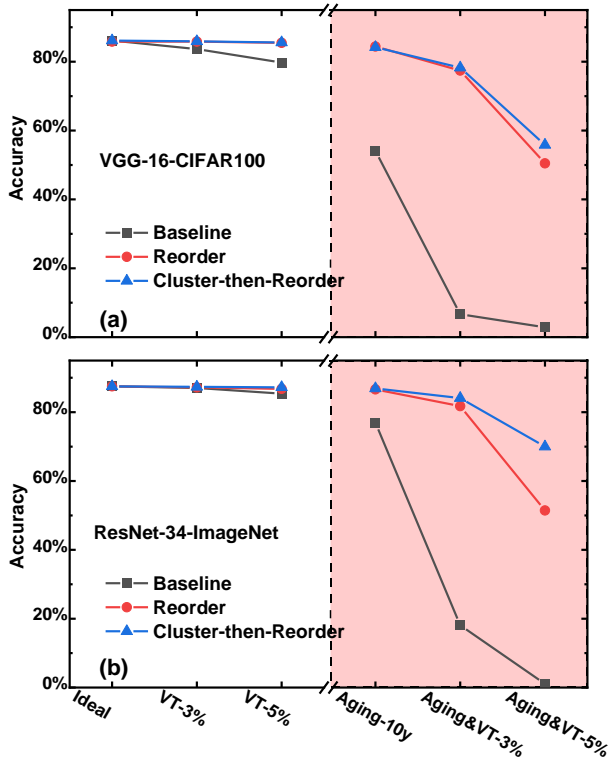


Fig. 11: Top-3 accuracy of (a) VGG-16 on CIFAR100 and (b) ResNet-34 on ImageNet under various PVTA conditions with different optimization techniques.

Fig. 10 shows the accuracy of VGG-16 and ResNet-18 on CIFAR10 under various PVTA conditions with different optimization algorithms. The accuracy loss of the baseline setting without any optimization is significant with the PVTA variations, especially after 10-year aging. While the accuracy of the proposed reordering algorithm and cluster-then-reorder algorithm is kept in an acceptable range.

Fig. 11 shows the top-3 accuracy of VGG-16 on CIFAR100 and ResNet-34 on ImageNet under various PVTA conditions. The trend is similar to Fig. 10. To speed up the simulation, we injected errors only into several vulnerable layers (those closer to the inputs). Although the proposed algorithm shows accuracy loss under extreme fluctuations, it still withstood a wider range of fluctuations compared to the baseline.

The proposed reordering algorithm can be adopted not only to improve the robustness of accelerators against PVTA variations, but also to optimize power consumption. A promising technique for low-power accelerators, timing speculation, uses Razor flip-flops for detecting and recovering timing errors. However, the detection and correction of timing errors by Razor flip-flops also cause significant power consumption. Without an appropriate design methodology, timing speculation can lead to additional power consumption that negates much of the energy efficiency gains achieved by operating at lower voltages. The proposed reordering algorithm in this paper can also reduce the toggle rate of Razor flip-flops in timing speculation accelerators, and allow for more aggres-

sive voltage scaling while maintaining acceptable inference accuracy, resulting in higher energy efficiency.

VI. CONCLUSION

In this paper, we present READ, a reliability-enhanced accelerator dataflow optimization algorithm. With the proposed output channels clustering and input channels reordering algorithm, the TER of the datapath can be significantly reduced. Evaluation with VGG and ResNet neural networks shows that the proposed methods can reduce TER by an average of $7.8\times$ and up to $37.9\times$, and make the accelerator more robust to PVTA variations, which demonstrates significant potential in reliable and efficient neural network accelerator design.

ACKNOWLEDGEMENTS

This work was supported in part by the NSFC (62125401, T2293700, T2293704) and the 111 Project (B18001)

REFERENCES

- [1] S. Tang *et al.*, "Robustart: Benchmarking robustness on architecture design and training techniques," *arXiv preprint arXiv:2109.05211*, 2021.
- [2] C. Liu *et al.*, "Fault-tolerant deep learning: A hierarchical perspective," *arXiv preprint arXiv:2204.01942*, 2022.
- [3] P. H. Hochschild *et al.*, "Cores that don't count," in *Proceedings of the Workshop on Hot Topics in Operating Systems*, 2021, p. 9–16.
- [4] H. D. Dixit *et al.*, "Silent data corruptions at scale," *arXiv preprint arXiv:2102.11245*, 2021.
- [5] M. Shafique *et al.*, "Robust machine learning systems: Challenges, current trends, perspectives, and the road ahead," *IEEE Design & Test*, vol. 37, no. 2, pp. 30–57, 2020.
- [6] P. N. Whatmough, S. K. Lee, D. Brooks, and G.-Y. Wei, "Dnn engine: A 28-nm timing-error tolerant sparse deep neural network processor for iot applications," *IEEE Journal Solid-State Circuits*, vol. 53, no. 9, pp. 2722–2731, 2018.
- [7] J. Zhang, K. Rangineni, Z. Ghodsi, and S. Garg, "Thundervolt: Enabling aggressive voltage undervolting and timing error resilience for energy efficient deep learning accelerators," in *ACM/IEEE Design Automation Conference (DAC)*, 2018.
- [8] X. Jiao, M. Luo, J. H. Lin, and R. K. Gupta, "An assessment of vulnerability of hardware neural networks to dynamic voltage and temperature variations," in *IEEE/ACM International Conference on Computer-Aided Design (ICCAD)*, 2017, pp. 945–950.
- [9] N. D. Gundi *et al.*, "Effort: A comprehensive technique to tackle timing violations and improve energy efficiency of near-threshold tensor processing units," *IEEE Transactions on Very Large Scale Integration Systems (TVLSI)*, vol. 29, no. 10, pp. 1790–1799, 2021.
- [10] P. Pandey, P. Basu, K. Chakraborty, and S. Roy, "Greentpu: Improving timing error resilience of a near-threshold tensor processing unit," in *ACM/IEEE Design Automation Conference (DAC)*, 2019, pp. 1–6.
- [11] K. Zhao *et al.*, "Ft-cnn: Algorithm-based fault tolerance for convolutional neural networks," *IEEE Transactions on Parallel and Distributed Systems (TPDS)*, vol. 32, no. 7, pp. 1677–1689, 2021.
- [12] D. Filippas, N. Margomenos, N. Mitianoudis, C. Nicopoulos, and G. Dimitrakopoulos, "Low-cost online convolution checksum checker," *IEEE Transactions on Very Large Scale Integration Systems (TVLSI)*, vol. 30, no. 2, pp. 201–212, 2022.
- [13] C. Schorn, A. Guntoro, and G. Ascheid, "An efficient bit-flip resilience optimization method for deep neural networks," in *IEEE/ACM Proceedings Design, Automation and Test in Europe (DATE)*, 2019, pp. 1507–1512.
- [14] F. Libano *et al.*, "Selective hardening for neural networks in fpgas," *IEEE Transactions on Nuclear Science*, vol. 66, no. 1, pp. 216–222, 2019.
- [15] N. D. Gundi *et al.*, "Effort: Enhancing energy efficiency and error resilience of a near-threshold tensor processing unit," in *IEEE/ACM Asia and South Pacific Design Automation Conference (ASPDAC)*, 2020, pp. 241–246.

- [16] T. Jia, Y. Ju, and J. Gu, "A dynamic timing enhanced dnn accelerator with compute-adaptive elastic clock chain technique," *IEEE Journal Solid-State Circuits*, vol. 56, no. 1, pp. 55–65, 2021.
- [17] Z. Du *et al.*, "Shidiannao: Shifting vision processing closer to the sensor," in *IEEE/ACM International Symposium on Computer Architecture (ISCA)*, 2015, pp. 92–104.
- [18] Y.-H. Chen, T. Krishna, J. S. Emer, and V. Sze, "Eyeriss: An energy-efficient reconfigurable accelerator for deep convolutional neural networks," *IEEE Journal Solid-State Circuits*, vol. 52, no. 1, pp. 127–138, 2017.
- [19] N. P. Jouppi *et al.*, "In-datacenter performance analysis of a tensor processing unit," in *IEEE/ACM International Symposium on Computer Architecture (ISCA)*, 2017, pp. 1–12.
- [20] V. Sze, Y.-H. Chen, T.-J. Yang, and J. S. Emer, "Efficient processing of deep neural networks: A tutorial and survey," *Proceedings of the IEEE*, vol. 105, no. 12, pp. 2295–2329, 2017.
- [21] B. Reagen *et al.*, "Ares: A framework for quantifying the resilience of deep neural networks," in *ACM/IEEE Design Automation Conference (DAC)*, 2018, pp. 1–6.
- [22] R. Huang *et al.*, "Variability-and reliability-aware design for 16/14nm and beyond technology," in *IEEE International Electron Devices Meeting (IEDM)*, 2017, pp. 12.4.1–12.4.4.
- [23] D. Ernst *et al.*, "Razor: a low-power pipeline based on circuit-level timing speculation," in *IEEE/ACM International Symposium on Microarchitecture (MICRO)*, 2003, pp. 7–18.
- [24] J. Pool and C. Yu, "Channel permutations for n:m sparsity," in *Advances in Neural Information Processing Systems*, vol. 34, 2021, pp. 13 316–13 327.
- [25] M. Martins *et al.*, "Open cell library in 15nm freepdk technology," in *IEEE International Symposium on Quality Electronic Design (ISQED)*. New York, NY, USA: Association for Computing Machinery, 2015, p. 171–178.
- [26] Z. Zhang, Z. Guo, Y. Lin, R. Wang, and R. Huang, "Avatar: An aging- and variation-aware dynamic timing analyzer for application-based dvafs," in *ACM/IEEE Design Automation Conference (DAC)*, 2022, p. 841–846.
- [27] S. Guo *et al.*, "Towards reliability-aware circuit design in nanoscale finfet technology: — new-generation aging model and circuit reliability simulator," in *IEEE/ACM International Conference on Computer-Aided Design (ICCAD)*, 2017, pp. 780–785.